EACWE2022

8th European-African Conference on Wind Engineering

20-23 September 2022 | Bucharest, Romania

Effects of barriers and angle of attack on the vortex-induced vibration of non-streamlined bridge decks

Bernardo Nicese[1*], Antonino Maria Marra[1)], Gianni Bartoli[1)], Claudio Mannini[1)]

1) CRIACIV - Department of Civil and Environmental Engineering, University of Florence, Florence, Italy, bernardo.nicese@unifi.it, antoninomaria.marra@unifi.it, gianni.bartoli@unifi.it, claudio.mannini@unifi.it

ABSTRACT: A study about vortex-induced vibration (VIV) of bridge decks was carried out, with special attention to the influence of section geometric details and wind angle of attack on VIV response, including a work about mathematical modeling of the phenomenon. Static and aeroelastic wind tunnel tests were performed on a bridge deck sectional model. Barriers and angles of attack gave rise to a variety of lock-in curves, in terms of onset flow velocity, curve shape and response amplitude. Results were employed to calibrate and assess two mathematical approaches for VIV modeling. Special attention was paid to peak amplitude prediction and the fluctuating lift force correlation increase with vibration amplitude was discussed.

Keywords: VIV, bridge decks, wind tunnel tests, traffic barriers, mathematical modeling

1. INTRODUCTION

Vortex-induced vibration represents a quite typical problem for bridge decks, especially in the case of slender bridges with limited mass per unit length and low natural frequencies. This phenomenon can cause non-negligible oscillations, even for limited values of the wind velocity, with consequent discomfort for users and possible fatigue damages to the structure. The aeroelastic response of a bridge can be strongly affected not only by the main geometry of the deck (Shiraishi and Matsumoto, 1983) but also by minor details and additions, such as the presence of lateral barriers or screens (Larsen and Wall, 2012). The flow angle of attack is also crucial for the aeroelastic behaviour of bridge decks (Kubo et al., 2002) and its variation can modify the response of the bridge in a similar way to an alteration of deck geometry. Starting from a representative bridge cross-section geometry, effects produced by two different traffic barriers are investigated over a realistic range of flow angles of attack through wind tunnel tests. Marked differences in the response of the structure caused by these elements are pointed out. Wind tunnel test results are also employed to assess the performance of two VIV mathematical models: a wake-oscillator model (Tamura and Matsui, 1979; Mannini et al., 2018) and a simple harmonic model (Marra et al., 2017). Model parameters are calibrated by means of test results and mathematical predictions are compared to wind tunnel experiments to discuss virtues and limitations of the models.

2. WIND TUNNEL TESTS

2.1. Bridge deck sectional model

The aluminium sectional model employed for the wind tunnel campaign is inspired by the Volgograd Bridge deck (Figure 1), which showed serious problems due to VIV and, in 2010, it was closed to traffic because of large vortex-induced vibrations, up to 80 cm of peak-to-peak amplitude. The sectional model is scaled with a factor of about 1:70 compared to the prototype, thereby

*) *Corresponding author*

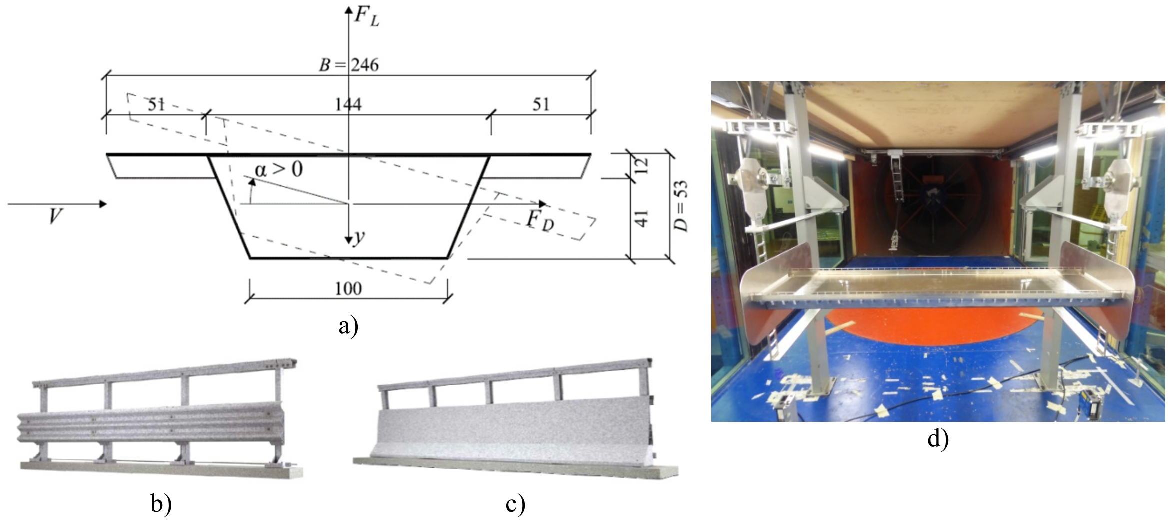

Figure 1. Wind tunnel model cross section (a); lateral traffic barrier typologies selected for experimental tests (b, c); sectional model installed on wind tunnel setup for the experimental campaign (d).

complying with the wind tunnel size, and it is 1 m long (L), 246 mm wide (B) and 53 mm deep (D). End-plates are provided at both ends of the model to confine the flow. Two realistic typologies of lateral barriers are considered (Figure 1(b, c)), so that the influence of these non-structural additions on the aerodynamic and aeroelastic behaviour of the bridge can be investigated. Their height is approximately equal to 40% of bare deck cross-flow dimension, while opening dimension and distribution are considerably different. The degree of transparency to the flow of Barrier 1 (Figure 1(b)) and Barrier 2 (Figure 1(c)) is respectively 51% and 23%.

2.2. Experimental results

Aerodynamic force measurements were firstly carried out through high frequency force balances connected to both ends of the sectional model. Static tests were performed for two Reynolds number values Re = 19000 and Re = 100000, with $Re = VD/\nu$ where V is mean wind speed and ν is air kinematic viscosity. Drag (C_D) and lift (C_L) coefficients were evaluated for different angles of attack (α) to describe bridge section aerodynamics and they were also employed for the calculation of the aerodynamic transverse force coefficient $C_{Fy}(\alpha) = -\sec(\alpha)\ [C_L(\alpha) + C_D(\alpha)\tan(\alpha)]$ (Figure 2(a)). C_{Fy} slope is related to the stability against transverse oscillation from a quasi-steady point of view. Lateral barriers enlarge the angle of attack range characterized by a positive slope and, hence, by a lower transverse stability according to quasi-steady theory. At the same time, the lift force spectrum was analysed to identify the Strouhal number (St) for different section layouts and it was integrated around Strouhal frequency to estimate the amplitude of the lift coefficient fluctuation due to vortex shedding (C_{L0}). St and C_{L0} were firstly estimated to describe the vortex-shedding force acting on the body. Barriers generate an increase of C_{L0}, suggesting a greater vortex-shedding intensity, and a reduction of St. Table 1 reports the main static test results corresponding to three realistic wind angles of attack for bridge deck investigation (0°, -3°, 3°). At the same time, C_{Fy}, $dC_{Fy}/d\alpha$, St and C_{L0} are aerodynamic parameters for the two mathematical approaches previously mentioned. In the second phase of the experimental campaign, aeroelastic tests were performed. The sectional model, suspended on an elastic dynamic setup (Figure 1(d)) with a natural oscillation frequency n_0 and allowing only the transverse degree of freedom, was left free to vibrate under the wind action. The response curves were achieved in terms of dimensionless transverse vibration amplitude Y, normalized with respect to the cross-flow dimension D. Different Scruton number values of the system ($Sc = 4\pi m\zeta_0/\rho BD$, where m is the oscillating mass per unit length, ζ_0 is the mechanical damping ratio, ρ is the air density) were tested by employing magnetic dampers to set different mechanical damping values. The lock-in curve (Figure 3(b)) was described with and without lateral barriers at -3°, 0° and 3° angles of attack, with large and, in some cases, unexpected effects due to barriers. On the other hand, free-decay tests at various values of reduced wind speed ($U = V/n_0D$) were carried out for all section configurations with the model elastically suspended.

Table 1. Transverse force coefficient slope ($dC_{Fy}/d\alpha$), Strouhal number (St), and dimensionless vortex-shedding force amplitude (C_{L0}) for different section layouts at different flow angles of attack.

Geometric configuration	α [deg]	$dC_{Fy}/d\alpha$ [-]	St [-]	C_{L0} [-]
Bare deck	0	-29.2	0.146	0.24
	-3	-15.9	0.147	0.23
	3	-18.9	0.133	0.19
Barrier 1	0	-25.8	0.122	0.40
	-3	-28.2	0.119	0.33
	3	-4.2	0.121	0.30
Barrier 2	0	-15.3	0.111	0.31
	-3	-40.7	0.104	0.42
	3	13.8	0.113	0.37

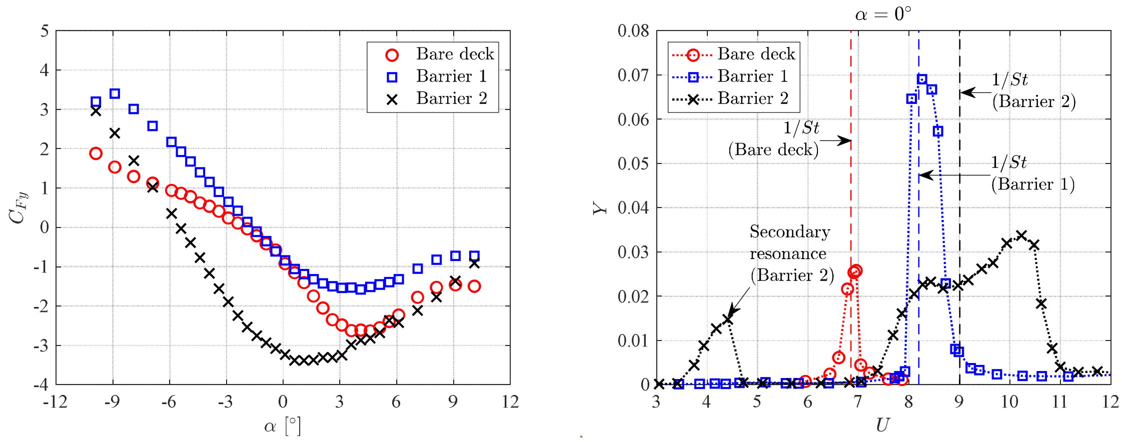

a) b)

Figure 2. Static and aeroelastic test results: aerodynamic transverse force coefficient (a), for Re = 19000, and response curve, in terms of transverse oscillation amplitude against reduced flow speeds, at zero angle of attack (b), for $3 \leq Sc \leq 4$.

These tests were performed outside the lock-in range and they were mainly aimed to estimate the aerodynamic damping, achieved as the difference between the damping value at a certain value of U and the mechanical one ζ_0. The aerodynamic damping experimentally estimated was compared to the one calculated according to the quasi-steady theory. A satisfying agreement between them was found in the case of negative slope and relatively linear trend of the C_{Fy} curve, both at low and high reduced wind velocity. Such a comparison was carried out in a mathematical modelling context. Both investigated models include indeed a quasi-steady contribution coming from the aerodynamic transverse force coefficient C_{Fy}.

3. MATHEMATICAL MODELING

Tamura-type wake-oscillator model was applied to determine the lock-in curves for each layout (Figure 3(a)). As above mentioned, a part of model parameters were estimated through static tests, while the remaining ones were calibrated by fitting aeroelastic response curves at low Sc. The equations of the model were found able to reproduce a variety of lock-in curve shapes, depending on parameter values. At the same time, the peak response was found to be mainly influenced by C_{L0} and an underestimation of the maximum vibration amplitude was generally found (Figure 3(b)). Harmonic model is a linear one-degree of freedom approach, and it can be employed only for peak response prediction. The model was fully calibrated through static test results and it was able, under certain conditions, to provide a good approximation of wake-oscillator model maximum amplitude. Generally, the underestimation of the prediction compared to experiments was even more marked for this second approach. It is worth mentioning that the increase of vortex-shedding

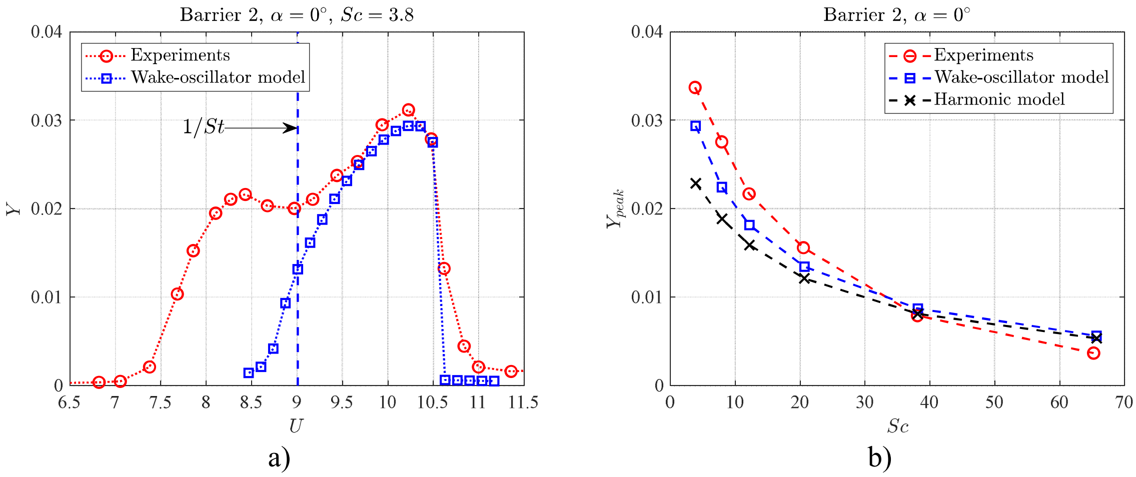

Figure 3. Experimental lock-in curve compared to wake-oscillator model prediction (a). Peak response amplitude against Scruton number for experiments and mathematical models (b).

force spanwise correlation (Ruscheweyh, 1990) in lock-in conditions was not taken into account, since the value of C_{L0} estimated through static force measurements was employed. An underestimation of the lift force acting on the vibrating body and, consequently, of the predicted response amplitude was therefore certainly possible. Pressure measurements should be performed on the oscillating model. In this context, as a very simplified approach, the sectional value of the vortex-shedding force for the stationary body could be extended to the whole model assuming full correlation at lock-in.

4. CONCLUSIONS

Wind tunnel static tests were able to give qualitative indications about the increased proneness to transverse vibration and VIV sensitivity in presence of barriers, as expectable. On the other hand, variations in barrier transparency to the wind may change completely the lock-in curve in terms of velocity range and vibration amplitude. This effect can be enhanced by a limited variation of the angle of attack, able to produce large changes in the bridge deck response. Opening distribution may indeed be more critical than barrier height for VIV response over a realistic angle of attack range. With regard to mathematical modeling, the wake-oscillator model can reproduce different lock-in curve typologies and the aerodynamic parameters were found to influence specific features of the predicted response. Both models are particularly sensitive to vortex-shedding force amplitude (C_{L0}) in terms of peak response prediction. In this context, a possibly marked increase of the vortex spanwise correlation with oscillation amplitude should be considered.

References

Kubo Y., Kimura K., Sadashima K., Okamoto Y., Yamaguchi E., Kato K. (2002). Aerodynamic performance of improved shallow π shape bridge deck. Journal of Wind Engineering and Industrial Aerodynamics, 90, 2113-2125.

Larsen A., Wall A. (2012). Shaping of bridge box girders to avoid vortex shedding response. Journal of Wind Engineering and Industrial Aerodynamics, 104-106, 159-165.

Mannini C., Massai T., Marra A. M. (2018). Modeling the interference of vortex-induced vibration and galloping for a slender rectangular prism. Journal of Sound and Vibration, 419, 493-509.

Marra A. M., Mannini C., Bartoli G. (2017) Modeling of vortex-induced vibrations of an elongated rectangular cylinder through wake-oscillator models. Proceedings of the 7th European African Conference on Wind Engineering, EACWE.

Ruschweyh H. (1990). Practical experiences with wind-induced vibrations. Journal of Wind Engineering and Industrial Aerodynamics, 33, 211-218.

Shiraishi N., Matsumoto M. (1983). On classification of vortex-induced oscillation and its application for bridge structures. Journal of Wind Engineering and Industrial Aerodynamics, 14, 419-430.

Tamura Y., Matsui G. (1979). Wake-oscillator model of vortex-induced oscillation of circular cylinder. Proceedings of the Fifth International Conference on Wind Engineering, (p. 1085-1094). Fort Collins, Colorado, USA.